ELSEVIER

Thermochimica Acta 250 (1995) 85–96

thermochimica acta

The thermal dehydration of $Na_2WO_4 \cdot 2H_2O$

Giulio G.T. Guarini *, Luigi Dei

Laboratory of Physical Chemistry of Interphases, Chemistry Department, University of Florence, Via G. Capponi 9, I-50121 Florence, Italy

Received 1 March 1994; accepted 22 June 1994

Abstract

The thermal dehydration in flowing dry nitrogen of commercial crystalline powders and of laboratory prepared single crystals of sodium tungstate dihydrate has been studied by power compensation DSC (both isothermal and dynamic runs) and optical microscopy. The two water molecules are lost in a single thermal event ending below 373 K in dynamic runs at scan speeds β lower than 1 K min^{-1}. Kinetic analysis of both types of thermal curve indicates that a partial transformation precedes the main decomposition for which the contracting circle equation is the best fitting one. Supporting evidence is drawn from optical microscopy which, however, also shows the formation and growth of randomly distributed nuclei on the single crystal surfaces. Furthermore, optical microscopy reveals that in some instances the observed surfaces undergo reorganization at the very beginning of nucleation. This indicates that a role is played in the decomposition by the interphasal zones of the crystals and is in agreement with recent findings on dehydration of other hydrates. Thermal data and kinetic parameters are reported and the mechanism of dehydration discussed.

Keywords: Decomposition; Dehydration; Kinetics; Sodium tungstate; Surface

1. Introduction

Sodium tungstate dihydrate is used in the preparation of coated electrodes for electrocatalysis [1] and as fire retardant for fabrics [2]. Its crystal morphology can be found in the Groth treatise [3], while its lattice constants and space group have

* Corresponding author.

SSDI 0040-6031(94)01944-C

been evaluated by Pistorius and Sharp [4]. Structure determination was performed by Mitra and Verma [5] and shows that the crystals pertain to the *Pbca* space group with $a = 8.454$ Å, $b = 10.598$ Å, $c = 13.895$ Å and 8 molecules in the unit cell. The thermal behaviour of sodium tungstate dihydrate heated up to 1273 K at $\beta = 10$ K min^{-1} was studied by Erdey et al. [6], while Gadalla et al. [2] reported that the dehydration takes place in a single step at low β but in two steps at $\beta > 10$ K min^{-1} indicating that at high heating rates, "the rate of evaporation is less than the rate of evolution of water"; the reported activation energy for low scan rates was 25.6 kJ mol^{-1}.

The present experimental study of the thermal decomposition of sodium tungstate dihydrate was undertaken with the principal aim (beyond the one of filling an apparent gap in the literature) of ascertaining if also the present reaction could be interpreted in terms of a recently proposed three-stage mechanism [7] in view of its possible extension to the decomposition reactions of crystal hydrates in general.

2. Experimental

The Merck pro analysi $Na_2WO_4 \cdot 2H_2O$ preferentially employed in the thermal runs consisted of thin plates (breadth about 0.8 mm) that could also have been used for microscope work if their surfaces had been less spoiled by recrystallization. The preparation of single crystals of sodium tungstate dihydrate required some time; in fact (in contrast to most crystal hydrates) relatively large single crystals are not easily obtained by evaporation of aqueous solutions. To obtain material suitable for microscope work we found it expedient to close a 100 ml beaker, containing 60 ml of a warm nearly saturated solution of the Merck product, inside a larger glass vessel in the presence of an open test tube containing about 15 ml of 96% ethanol which, migrating through the gas phase to the tungstate solution, slowly decreases the solubility of the salt. In this way it was possible to collect (mainly at the beaker glass wall near the meniscus) millimetre size plates showing thicknesses of the order of about 300 μm. In agreement with previous structural and morphologic findings [3–5] these were identified as exposing the (001) plane. The crystalline material which precipitated at the bottom of the beaker consisted of much smaller and thinner platelets (average breadth about 70 μm with plates up to 200 μm, with thicknesses rather uniformly distributed in the range 7–11 μm) and was recovered separately and identified as "powder B". Single crystals and powder B were washed separately with 96% ethanol and then allowed to dry in air.

The thermal curves were recorded both in isothermal and dynamic modes using preferentially a power compensation Perkin-Elmer DSC7 differential scanning calorimeter using the default (In–Zn) calibration checked by the 343 K melting of biphenyl and the 398 K transition of NH_4NO_3. During the experiments the cell of the apparatus was always purged by dry nitrogen flowing at 16 ml min^{-1}. In the isothermal runs the purging flow was started only after reaching the temperature of the experiment. In dynamic runs, at scanning rates β in the range 0.1–16 K min^{-1},

10–13 mg of sodium tungstate dihydrate were weighed in the standard aluminium sample pans. Higher sample masses (16–20 mg) were used in the isothermal runs that were performed in the 323–338 K range. Lids were invariably added to sample and reference pans to loosely cover the sample and match the thermal emissivity [8]. Renewed weighing after runs allowed determination of the mass loss. The Perkin-Elmer software was used to evaluate both enthalpic changes and kinetic parameters from the dynamic thermal curves. However, the kinetic analysis of both types of curve was also performed by testing the best fit among the various kinetic laws [9] for isothermal runs and extracting from the data station the values of the fraction decomposed α, and of $d\alpha/dT$ to use a differential method [10] for dynamic runs. For the sake of comparison and to test for self-cooling [11] some dynamic experiments were also performed using a Mettler TA 2000 heat flux thermal analyzer under the same experimental conditions.

A Reichert Zetopan optical microscope equipped with interference contrast and with an Olympus OM2 camera was used in the reflection mode to follow the behaviour of the surfaces of single crystals allowed to decompose in the same flow of dry nitrogen as used in thermal runs. In these experiments a cell already described [12] was employed in which the sample temperature was monitored by a copper–constantane thermocouple lying, nearly in contact with the crystal, on the same supporting glass plate. For better comparison with dynamic experiments, the power supply to the resistance heating the whole cell was regulated so that rather constant heating rates of 1.5 to 2.5 K min^{-1} could be maintained in the temperature range of interest (323–373 K). Microscope experiments were usually continued up to the complete spreading of the product on the exposed (001) reactant surfaces; under the conditions of the experiments this happened at about 353 K. In some instances, in spite of fragility and very low thickness of the reacted crystals, it has been possible to cleave them perpendicularly to the reacted surfaces to observe and record the status of the new surfaces exposed on fracture.

3. Results

3.1. Isothermal experiments

The thermal curves of three runs performed with the Merck product at slightly different temperatures are collected in Fig. 1 (full lines) together with those of three runs performed with powder B (dashed lines). The initial splitting of the thermal curve indicative of separation of surface and bulk [13,14] appears as a shoulder in the former runs while it is well resolved in some powder B experiments because, we believe, both of the much higher surface perfection and the increased surface/bulk ratio of these samples.

3.1.1. Merck powders

The kinetic analysis of the curves indicated the contracting circle equation as being the best fitting one over almost the whole decomposition (Fig. 2). For these

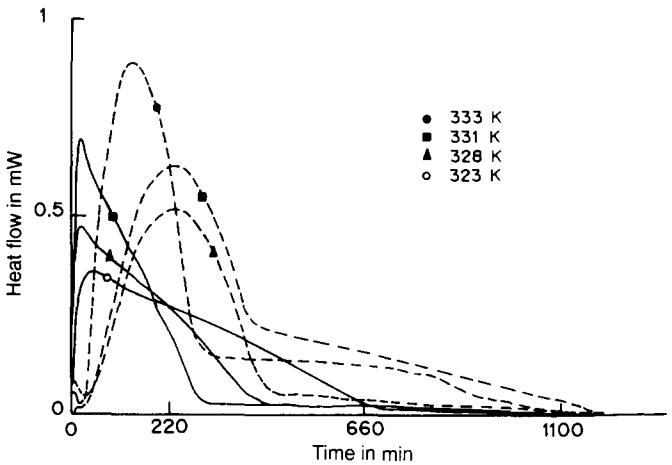

Fig. 1. Thermal curves for the isothermal dehydration of Merck (full line) and powder B (dashed line) samples.

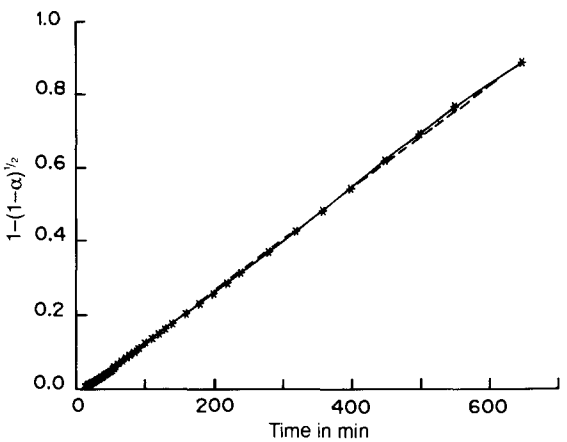

Fig. 2. Fitting of isothermal (323 K) data by the contracting circle equation (Merck samples).

runs reduced time plots (Fig. 3) ensured that a single mechanism was working. The kinetic parameters were evaluated as $E_a = 86.1 \pm 7.3$ kJ mol^{-1} and $\ln(A/s^{-1}) = 22.4 \pm 3.1$. It is to be noted that values about 1.5 times higher for E_a and about 1.7 times higher for ln A were deduced from the relatively short (up to 12 min) induction periods apparent because the plots of the type shown in Fig. 2 did not converge at the origin; these values compare with those typical of the acceleratory period found for powders B and in dynamic runs, and probably have the same explanation (vide infra).

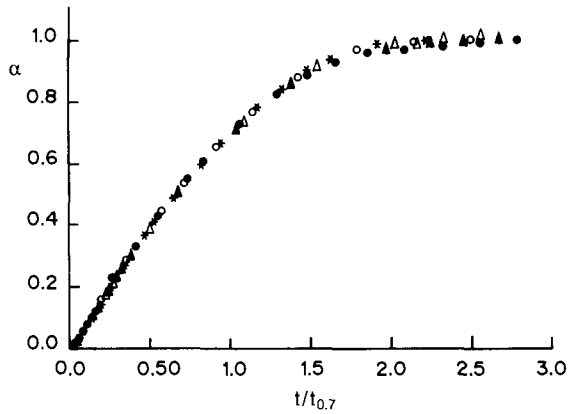

Fig. 3. Reduced time plot for a number of experiments with Merck material; ○, 323 K; *, 325 K; △, 328 K (a); ▲, 328 K (b); ●, 331 K.

3.1.2. Powders B

The kinetic analysis of these runs revealed that the thermal curves could not be fitted over the whole range of α by a single kinetic law (the best fit being an order of reaction type equation with $n = 1$ but with a very poor correlation coefficient). Consideration of the experiments by optical microscopy (see below) suggested that these runs could be better interpreted as consisting of two stages, namely an acceleratory stage followed by a decay stage. Microscopy indicated the decay stage as a contracting one and the analysis of the data again gave the contracting circle as the best fit in the $0.12 < \alpha < 0.88$ range while an $n = 2$ power law was found to apply for $\alpha < 0.12$. For this initial acceleratory stage the values of the activation parameters were: $E_a = 138.6 \pm 0.7$ kJ mol^{-1} and $\ln(A/s^{-1}) = 40.7 \pm 5.2$. For the main contracting stage the same kinetic parameters as found for Merck powder apply; in fact the experimental points can be plotted in the same Arrhenius diagram (Fig. 4).

3.2. Dynamic experiments

A thermogram (Fig. 5, full line), reputed to be typical of the decomposition, recorded at $\beta = 2$ K min^{-1} dehydration of 11.99 mg of Merck powders, is compared with the corresponding thermogram (Fig. 5, broken line) obtained using 10.2 mg of powder B. This second curve is narrower than the first one and is shifted some 10 K towards the higher temperatures; the shoulder clearly evident (at about 343 K) in the initial part of the first curve is, however, retained even if it is somewhat less evident. In both cases the dehydration takes place in a single event and appears to end at about 380 K; furthermore, the heat of reaction is unchanged irrespective of the nature of the sample. In the present experiments the overall shape of the curves remains the same up to $\beta = 16$ K min^{-1} and no splitting is evidenced at high β in disagreement with Ref. [7]. At $\beta < 1$ K min^{-1} the dehydration peaks

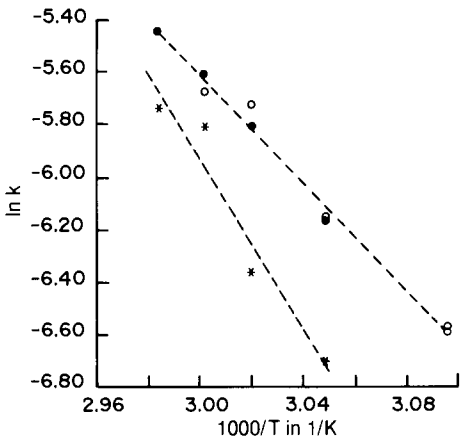

Fig. 4. Arrhenius plot for the isothermal decompostion of Merck (○) and powder B (●) samples. The values of the ln $(k - 0.7)$ for the initial $n = 2$ power law obedience (powder B) have also been added (*).

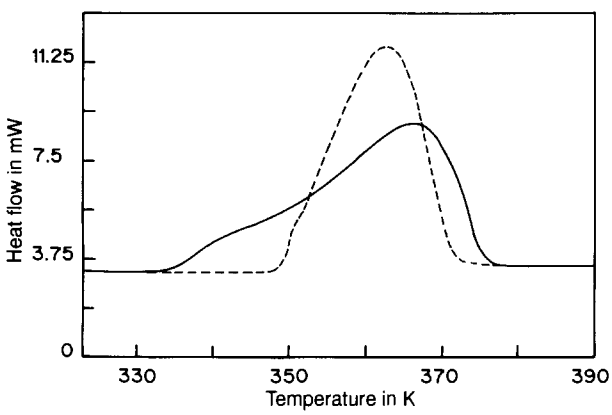

Fig. 5. Comparison of the dynamic ($\beta = 2$ K min^{-1}) behaviour of Merck (full line) and powder B (broken line) samples.

were observed to end below 373 K; in no instance did a decomposition end beyond 413 K. The mean value of the enthalpic change for the runs with $\beta \leqslant 8$ K min^{-1} is 345.3 ± 8.2 J g^{-1} (i.e. 56.9 kJ per mole of water, in good agreement with previous results of dehydration of crystal hydrates [15]).

Mass loss determinations showed that some water is retained in the product; in fact, in agreement with Ref. [6], the stoichiometric loss of 10.92% was reached only in a few test experiments at intermediate heating rates in which the temperature was pushed somewhat beyond 473 K. In the runs interrupted at the end of the thermal curve the loss never exceeded 10.55%, being just a little higher than 10% in runs with $\beta \geqslant 8$ K min^{-1}. This is reputed to be in agreement with Ref. [7] and was the reason for the exclusion of the latter runs (showing enthalpic changes of about 300 J g^{-1}) in the above evaluation of the heat of dehydration. Incidentally, water

retention is reputed to be responsible for the "tails" clearly evident in some isothermal experiments (Fig. 1).

The kinetic analysis of the dynamic thermograms of the Merck material, performed by the differential method successfully used previously [7,16,17], confirmed the overall ($0.03 < \alpha < 0.90$) obedience of the transformation to the contracting circle equation: a typical plot of $\ln\{d\alpha/dT[f(\alpha)]^{-1}\}$ versus $(T/K)^{-1}$ when $f(\alpha) = 2(1-\alpha)^{1/2}$ is shown in Fig. 6. From plots of this type activation energies and pre-exponential factors was deduced as $E_a = 87.8 \pm 7.3$ kJ mol^{-1} and $\ln(A/s^{-1}) = 25.6 \pm 2.7$ in good agreement with the values deduced from the isothermal runs. For the sake of comparison the kinetic parameters deduced from non-isothermal runs using the Perkin-Elmer software were $n = 0.56 \pm 0.06$, $E_a = 92.5 \pm 4.6$ kJ mol^{-1} and $\ln(A/s^{-1}) = 24.5 \pm 1.5$. For the range $0 < \alpha < 0.03$ an $n = 2$ power law proved effective with an activation energy some 30% higher than the latter one.

We wish to note here that the values we report for the activation energy of the main process are approximately four times that quoted in Ref. [2] which leads us to suspect a misprint (kJ in place of kcal) in that article. This is supported by the consideration that the activation energy of an endothermic process would otherwise be lower than the heat of transformation.

Both the differential method and the Perkin-Elmer software gave first order kinetics as the best fit over the whole range of α for powder B. The kinetic parameters evaluated by the differential method $\{f(\alpha) = 1-\alpha\}$ are $E_a = 144.6 \pm 8.3$ kJ mol^{-1} and $\ln(A/s^{-1}) = 45.4 \pm 4.2$; the corresponding Perkin-Elmer values are $n = 0.91 \pm 0.02$, $E_a = 136.1 \pm 13.2$ kJ mol^{-1} and $\ln(A/s^{-1}) = 40.2 \pm 5.3$. It is perhaps of some significance to note here that these values for E_a match that found for the acceleratory portion of the isothermal experiments. Furthermore the first order obedience is probably due to the very small size and thickness of the microcrystals constituting the type B powder samples [9,18].

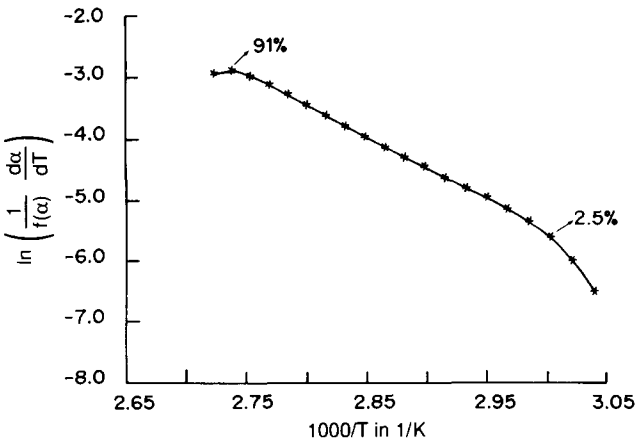

Fig. 6. Typical differential method plot obtained for a dynamic run using as $f(\alpha)$ the contracting circle expression.

3.3 Optical microscopy experiments

A sequence of micrographs recorded during the dehydration of a single crystal of $Na_2WO_4 \cdot 2H_2O$ in flowing nitrogen while the temperature increased at about 2 K min^{-1} is shown in Fig. 7. At about 343 K, circular nuclei appear on the observed {001} surfaces and subsequently (Fig. 7) expand laterally to occupy the whole

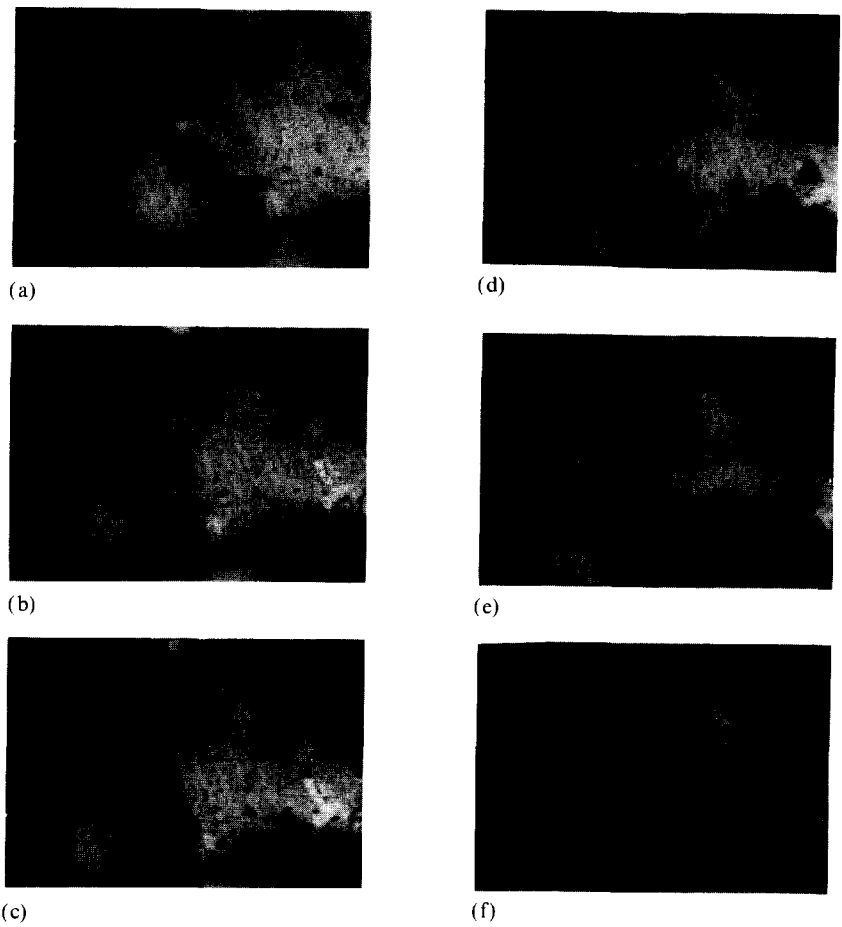

Fig. 7. Sequence of micrographs recorded during the dehydration of a single crystal in flowing N_2: nuclei are observed to appear between (b) and (c) and subsequently grow up to almost complete coverage of the crystal surface. (a) 292 K, (b) 336 K, (c) 346 K, (d) 349 K, (e) 351 K, (f) 353 K. Original magnification 86×.

Fig. 8. Sequence of micrographs of the dehydration of a single crystal showing surface retexturing at the beginning of product crystallization on the surface (nucleation). (a) 296 K, (b) 339 K, (c) 347 K, (d) 349 K, (e) 350 K, (f) 352 K, (g) 353 K, (h) 354 K, (i) 355 K, (j) 356 K. Original magnification 86×.

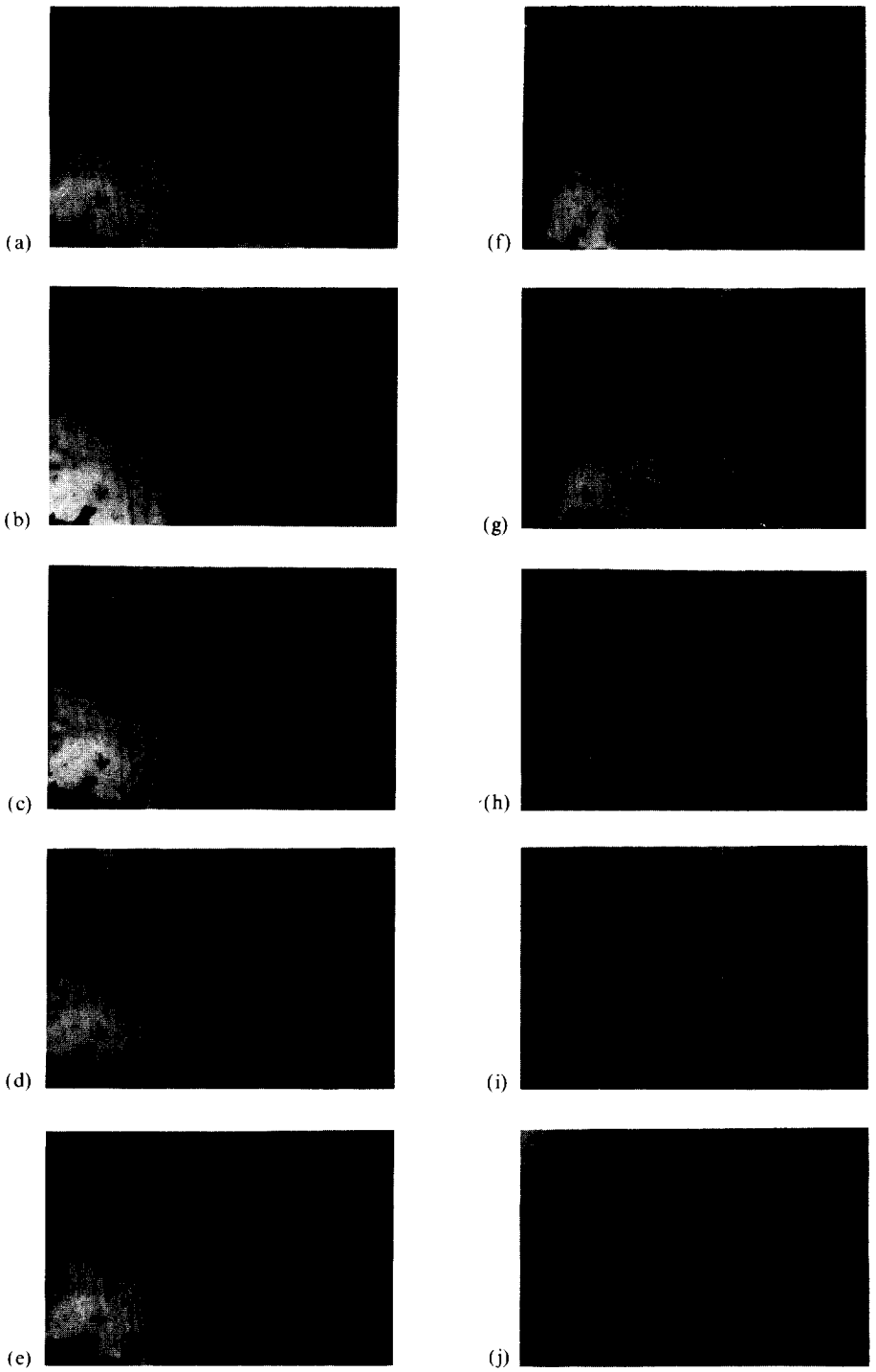
(a)
(b)
(c)
(d)
(e)
(f)
(g)
(h)
(i)
(j)

surface. It is perhaps of some importance that, after the initial appearance, the number of nuclei does not change significantly; this is evident in all the experiments performed.

Another sequence of micrographs, referring to the dehydration of a different crystal of the same batch under the same conditions, and reputed to be of particular signficance, is reported in Fig. 8. Evidence is found here that, almost comtemporaneously with the appearance of the nuclei, the surface observed undergoes a significant texture change; white striae appear (Fig. 8(d)) which, however, later disappear (Fig. 8(h)) from the zones uncovered by the growing nuclei.

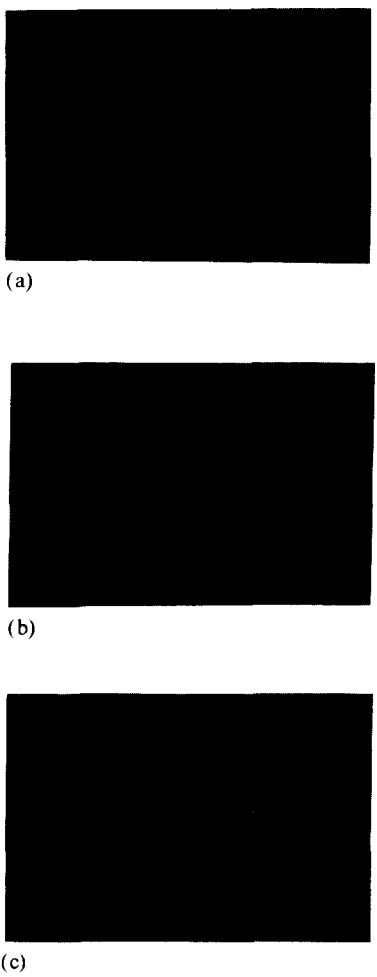

Fig. 9. Micrographs of the surfaces exposed on cleavage of crystals after completion of dehydration experiments in the microscope cell. During cleavage some product has spilled over the freshly exposed surfaces. The contracting envelope nature of the decomposition is evident. The crystal in Fig. 9(a) is the same as in Fig. 7. Original magnification 86×.

Some results of cleaving the crystals recovered from microscope experiments perpendicularly to the reacted surfaces are shown in Fig. 9. It is evident that when the outer surfaces are completely covered with the product the bulk remains unaltered, a situation typical of contracting envelope kinetics and which confirms the thermal results.

4. Discussion and conclusions

The results reported might take a hurried reader to the conclusion that the thermal dehydration of $Na_2WO_4 \cdot 2H_2O$ is a simple process taking place by a contracting envelope mechanism. This is only partly true. Indeed, if the contracting mechanism really explains the main part of the decomposition, a number of experimental findings (see below) indicate that the process is not so simple.

First of all the dehydration of sodium tungstate dihydrate shows a relevant sensitivity to the degree of perfection of the crystal surfaces. This is revealed by the delayed beginning of the main transformation in isothermal and dynamic runs found for recrystallized material that also shows the isothermal separation of surface and bulk reaction typical of surface sensitive materials [12–14].

It must then be taken into consideration that a true contracting envelope mechanism would require instantaneous nucleation while in the present instance the isothermal runs indicate the presence of an induction period, and microscopy shows the presence and growth of separate random nuclei; indeed, dynamic runs show that the contracting mechanism starts only after about 3% of the decomposition has already taken place. However, microscopic results confirm the contracting mechanism (Fig. 9) but also suggest (compare the temperature with that of the shoulder in Fig. 4) that the latter begins after the surface is completely covered by the product.

Another point concerns the change of texture of the crystal surfaces submitted to dehydration in the microscope cell. In agreement with the previous findings on different crystals [12,15,19,20], this reveals the initial formation on the surfaces of the crystals of a dehydrated layer that later begins to crystallize originating at the observed circular nuclei. In this particular case the layer appears to corrugate (striae) when the nuclei begin to form as if these exerted some lateral compression on the layer covering the intranuclear zones. Incidentally, the initial formation of a surface layer is also confirmed [7,13] by the small initial endotherm (corresponding to less than 1% reaction) observed during the isothermal dehydration of powder B samples. The permeability of the dehydrated layer to the reaction product is probably poor (high local product pressure and high activation energy of the induction period [21]) but improves as crystallization begins generating surface nuclei and introducing discontinuities in the layer [7]. This permeability (and consequently the reaction rate) is promoted by product crystallization and increases with the approximately two dimensional spreading of the nuclei on the surface. This explains the applicability of the $n = 2$ power law to the initial portions of the decompositions. When eventually the surface layer is completely crystallized and

the escape of the water released by the reaction is relatively complete, the transformation proceeds inward according to the contracting envelope mechanism. Some water molecules can however remain absorbed on product surfaces [16], this retention being proved by the results on mass loss and by the high temperature tail often observed also in the dynamic thermograms.

The considerations outlined above ensure that the present decomposition follows a mechanism identical to the three-stage one deduced for the dehydration of $\alpha NiSO_4 \cdot 6H_2O$ [7] and found effective also in the dehydration of alums [16] as well as in the decomposition of $NaHCO_3$ [17].

Such a mechanism shows the role (often neglected) of the interphases in the reactivity of crystals and we hope that further experimentation will reveal that it is much more general than the nucleation and growth mechanism in which the reaction is believed to take place at the boundaries of a nucleus.

Acknowledgements

The authors feel indebted to Dr. A.K. Galwey for his help in improving the presentation of this paper, to Mr. Paolo Parri and to Mr. Pierluigi Cresci for their help with illustrative material and electronic devices, respectively. Financial support from M.U.R.S.T. (60%) is acknowledged.

References

[1] P.J. Kulesza and L.R. Faulkner, J. Am. Chem. Soc., 110 (1988) 4905.
[2] A.M. Gadalla, M.F. Abadir, M.J. Kasem and F.T. Salem, AIChE J., 30 (1984) 50.
[3] P. Groth, Chemisches Krystallographie, Zweiter Teil, Verlag von Wilheim Engelman, Leipzig, 1908, p. 365.
[4] W.F.T. Pistorius and W.E. Sharp, Acta Crystallogr., 14 (1961) 316.
[5] R.P. Mitra and H.K.L. Verma, Indian J. Chem., 7 (1969) 598.
[6] L. Erdey, J. Simon, S. Gal and G. Liptay, Talanta, 132 (1966) 67.
[7] G.G.T. Guarini, J. Therm. Anal., 41 (1994) 287.
[8] G.G.T. Guarini, R. Spinicci and D. Donati, J. Therm. Anal., 6 (1974) 405.
[9] M.E. Brown, D. Dollimore and A.K. Galwey, Comprehensive Chemical Kinetics, Vol. 22, Elsevier, Amsterdam, 1980.
[10] J.H. Sharp amd S.A. Wentworth, Anal. Chem., 41 (1963) 2060.
[11] H. Tanaka and N. Koga, J. Therm. Anal, 36 (1990) 2601.
[12] G.G.T. Guarini and L. Dei, J. Chem. Soc. Faraday Trans. 1, 79 (1983) 1599.
[13] G.G.T. Guarini and M. Rustici, J. Therm. Anal., 34 (1988) 487.
[14] G.G.T. Guarini and S. Piccini, J. Chem. Soc. Faraday Trans. 1, 84 (1988) 331.
[15] L. Dei, G.G.T. Guarini and S. Piccini, J. Therm. Anal., 29 (1984) 755.
[16] A.K. Galwey and G.G.T. Guarini, Proc. R. Soc. London, A, Ser. 441 (1993) 313.
[17] G.G.T. Guarini, L. Dei and G. Sarti, J. Therm. Anal. in press.
[18] D.A. Young, Decomposition of Solids, Pergamon Press, Oxford, 1966.
[19] A.K. Galwey, R. Spinicci and G.G.T. Guarini, Proc. R. Soc. London, Ser. A, 378 (1981) 477.
[20] G.G.T. Guarini, Colloids Surf., 59 (1991) 83.
[21] M. Reading, D. Dollimore and R. Whitehead, J. Therm. Anal., 17 (1991) 2165.